Protonation status and control mechanism of flavin–oxygen intermediates in the reaction of bacterial luciferase

Ruchanok Tinikul[1] (iD), Narin Lawan[2], Nattanon Akeratchatapan[3], Panu Pimviriyakul[4], Wachirawit Chinantuya[1], Chutintorn Suadee[1], Jeerus Sucharitakul[5] (iD), Pirom Chenprakhon[6], David P. Ballou[7], Barrie Entsch[8] and Pimchai Chaiyen[1,3]

1 Department of Biochemistry and Center for Excellence in Protein and Enzyme Technology, Faculty of Science, Mahidol University, Bangkok, Thailand
2 Department of Chemistry, Faculty of Science, Chiangmai University, Thailand
3 School of Biomolecular Science and Engineering, Vidyasirimedhi Institute of Science and Technology (VISTEC), Rayong, Thailand
4 Department of Biochemistry, Faculty of Science, Kasetsart University, Bangkok, Thailand
5 Department of Biochemistry, Faculty of Dentistry, Chulalongkorn University, Bangkok, Thailand
6 Institute for Innovative Learning, Mahidol University, Nakhon Pathom, Thailand
7 Department of Biological Chemistry, University of Michigan, Ann Arbor, MI, USA
8 School of Science and Technology, University of New England, Armidale, NSW, Australia

Bacterial luciferase catalyzes a bioluminescent reaction by oxidizing long-chain aldehydes to acids using reduced FMN and oxygen as co-substrates. Although a flavin C4a-peroxide anion is postulated to be the intermediate reacting with aldehyde prior to light liberation, no clear identification of the protonation status of this intermediate has been reported. Here, transient kinetics, pH variation, and site-directed mutagenesis were employed to probe the protonation state of the flavin C4a-hydroperoxide in bacterial luciferase. The first observed intermediate, with a λ_{max} of 385 nm, transformed to an intermediate with a λ_{max} of 375 nm. Spectra of the first observed intermediate were pH-dependent, with a λ_{max} of 385 nm at pH < 8.5 and 375 at pH > 9, correlating with a pK_a of 7.7–8.1. These data are consistent with the first observed flavin C4a intermediate at pH < 8.5 being the protonated flavin C4a-hydroperoxide, which loses a proton to become an active flavin C4a-peroxide. Stopped-flow studies of His44Ala, His44Asp, and His44Asn variants showed only a single intermediate with a λ_{max} of 385 nm at all pH values, and none of these variants generate light. These data indicate that His44 variants only form a flavin C4a-hydroperoxide, but not an active flavin C4a-peroxide, indicating an essential role for His44 in deprotonating the flavin C4a-hydroperoxide and initiating chemical catalysis. We also investigated the function of the adjacent His45; stopped-flow data and molecular dynamics simulations identify the role of this residue in binding reduced FMN.

Introduction

Bacterial luciferase (Lux) is the only known flavin-dependent monooxygenase capable of generating light. Lux reactions catalyze the oxidation of long-chain aldehydes to corresponding acids using oxygen and reduced FMN and produce light with approximately 16% quantum yield [1,2]. Such bioluminescence has long been used for sensitive detection tools in biomedical, food, and environmental applications [3,4]. Among the characterized bioluminescent systems, Lux and fungi luciferases are the only such systems that all genes related to substrate regeneration are known [5–7]. This makes Lux system attractive for biomedical applications because by introducing the whole cassette of *luxCDABEG* genes into heterologous cell targets, it is possible to generate autoluminous cells resulting in potentially real-time monitoring and *in vivo* bio-imaging [8,9]. Recently, directed evolution has been used to improve the light brightness of the *lux* operon (seven-fold brightness increase compared with the native operon), which could achieve single-cell detection levels demonstrated in both bacterial and mammalian cells [10,11].

Lux is a heterodimeric enzyme consisting of α- and β-subunits encoded by *luxA* and *luxB* genes in the *lux* operon, respectively. The α-subunit is the major site for catalysis, while the β-subunit is thought to be required for supporting proper protein folding of the α-subunit into its active form. Crystal structures and functional analysis of Lux have confirmed the active site to be in the α-subunit [12–14]. Lux belongs to the class C of flavin-dependent monooxygenases that catalyzes incorporation of a single atom of oxygen into aldehyde to form the corresponding acid using the reactive flavin intermediate, flavin C4a-hydroperoxide (flavin C4a-OOH) [15–18]. The flavin reductase, encoded by *luxG*, catalyzes the reduction in FMN by NADH, and the resulting reduced FMN is transferred to Lux. Because the N1 of the reduced flavin ring has pK_a of 6.7, reduced FMN is represented as an anionic reduced flavin form, $FMNH^-$, which is the form that reacts with oxygen [19]. The binary complex of Lux: $FMNH^-$ reacts with oxygen to initially generate the flavin C4a-OOH intermediate. Current thinking is that the active flavin C4a-peroxide (flavin C4a-OO$^-$) intermediate reacts with aldehyde to form a flavin C4a-hemiacetal adduct. The O–O bond then breaks to produce the acid and an excited state of the C4a-hydroxyflavin that liberates light as it relaxes to the ground state (Scheme 1) [20–22].

Because the protonation status of the flavin C4a-OOH is likely to be a major factor for determining whether it will act as an electrophile or a nucleophile [17,23,24], understanding the protonation status of intermediates at various stages of catalysis is important for understanding the mechanism of oxygen transfer and would be useful for future enzyme engineering to fine-tune desired activities. Flavin-dependent monooxygenases that transfer a –OH to nucleophilic phenolic substrates use an electrophilic protonated flavin C4a-OOH [25,26]. The Baeyer–Villiger monooxygenases (BVMOs) (and likely Lux) use the more nucleophilic deprotonated flavin C4a-OO$^-$ to attack and ultimately incorporate oxygen into the substrate [27,28]. Although for Lux it is generally proposed that the flavin C4a-OO$^-$ is involved in a nucleophilic attack of the aldehyde, identification of the protonation status of Lux intermediates has never been reported. It was not clear whether flavin C4a-OOH first forms before deprotonation occurs to result in the flavin C4a-OO$^-$ or whether the enzyme directly forms flavin C4a-OO$^-$. For the oxygenase component of *p*-hydroxyphenylacetate hydroxylase (C$_2$) in which a flavin C4a-OOH is required to act as an electrophile, experimental and computational results indicate that a flavin C4a-OOH is the first intermediate to form. The reduced flavin reacts with molecular oxygen via a concerted process of proton-coupled electron transfer to initially generate a radical pair of the flavin semiquinone and a protonated superoxide anion, which then collapses to form the flavin C4a-OOH adduct [29,30]. A similar proton-coupled electron transfer process to generate the flavin C4a-OOH was also observed in the reaction of pyranose 2-oxidase (P2O), an oxidase that can form flavin C4a-OOH [31]. In both enzymes, the active site His located close to the C4a position of the flavin ring (ca. 4.5–4.6 Å) [32] is the key residue that provides a proton for the proton-coupled electron transfer process to generate the flavin C4a-OOH intermediate. Based on the active site architecture of Lux, two active site His residues (His44 and His45) are located close to the pyrimidine moiety on the *si*-side of the isoalloxazine ring (~ 7.5 Å to C4a position, in the case of His44) (Fig. 1A) [12]. Recently, by using computational calculations, Luo and Liu [33] have proposed that the flavin C4a-OOH formation in Lux also proceeds via a proton-coupled electron transfer mechanism, in which His44 is the proton provider. It is possible that a flavin C4a-OOH is the first species to form before it deprotonates to form flavin the C4a-OO$^-$ that nucleophilically attacks the aldehyde. However, none of the experimental results have assigned the protonation forms of this intermediate in Lux.

For the reactions of the Baeyer–Villiger enzyme, cyclohexanone monooxygenase (CHMO), in which
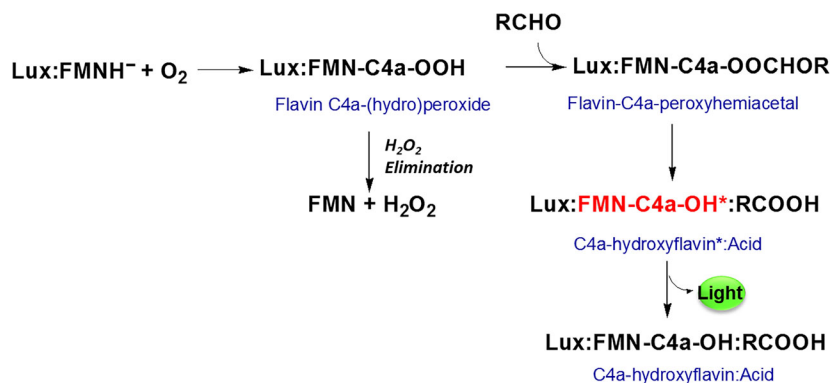
Scheme 1. The reaction mechanism of Lux proceeds via formation of flavin-C4a-OOH intermediates.
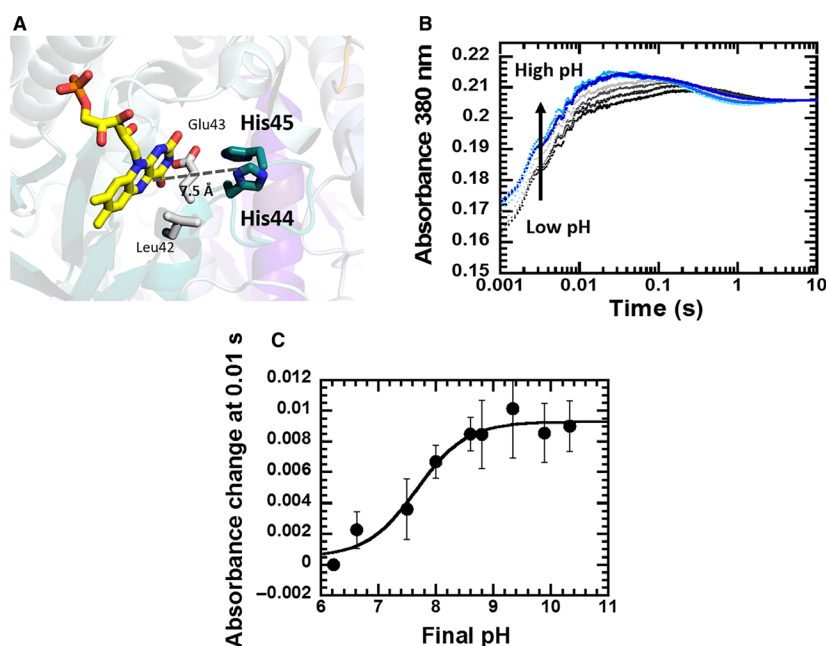

Fig. 1. (A) An active site of Lux with oxidized FMN bound (PDB: 3FGC) created by PYMOL program (Schrödinger Inc., New York, NY, USA) shows the conserved His44 located near the C4a position of the isoalloxazine ring. (B) The kinetic traces monitored at 380 nm of the reaction of reduced wild-type Lux (Lux:FMNH$^-$) and oxygen at various pH values. Solutions of 80 μM Lux and 16 μM FMNH$^-$ in 10 mM sodium phosphate buffer pH 7.0 were mixed with oxygen (0.13 mM) in buffers at various pH values at 4 °C. Concentrations are given as final concentrations after mixing. (C) A plot of absorbance 380 nm changes observed at 0.01 s from (B) *versus* final pH. A pK_a value of 7.7 ± 0.17 was calculated from three replicate experiments and presented as mean ± standard deviation.

flavin C4a-OO$^-$ is required to act as a nucleophile, stopped-flow experiments performed at various pH values were used to probe the protonation status of flavin intermediates. Results indicated that the flavin C4a-OO$^-$ was the first intermediate to form in the CHMO reaction, and this intermediate was also identified as the one incorporating an oxygen atom into cyclohexanone [34]. For another BVMO, phenylacetone monooxygenase, the H-bonding interactions between NAD(P)H and the guanidinium group of the active site Arg with the flavin isoalloxazine N5 position were proposed to be important for stabilizing the flavin C4a-OO$^-$ [28,35]. There was also a report from studies of phenylacetone monooxygenase from *Thermobifida fusca* of a mutation of a residue (Cys65) nearby the flavin ring that resulted in converting this

BVMO to an NADPH oxidase. Alteration from Cys65 to Asp resulted in a different side chain orientation that caused steric hindrance, thus preventing oxygenation and favoring decay of the intermediate into oxidized flavin and H$_2$O$_2$ [36]. For the Lux reaction, the factor controlling the intermediate protonation status is currently unknown. Previous site-directed mutagenesis studies of His44 and His45 in Lux from *Vibrio harveyi* reported that bioluminescence levels of His44Ala and His45Ala variants were 6–7 orders of magnitude less than that of the wild-type enzyme [37–39]. Although it was concluded that these His44 and His45 residues should be important for the generation of light-emitting species, the exact functional roles of these residues are not fully understood. Understanding how His44 and His45 are important for the reaction

catalyzed by Lux would be useful for future optimization and engineering of Lux.

In this study, to better assign the protonation status of intermediates, transient kinetics studies of the Lux reaction were carried out to identify changes in the spectral properties of flavin intermediates as a function of pH. Stopped-flow data from the reaction of O_2 with $FMNH^-$ in complex with Lux indicate that the flavin C4a-OOH is the first species observed, while the flavin C4a-OO$^-$ forms later. Similar experiments showed that His44 variants cannot generate light-emitting species and that the flavin C4a-OOH formed in these variants remained protonated without forming flavin C4a-OO$^-$ at most of pH values investigated. The His45 variants cannot bind $FMNH^-$ effectively, and this property was corroborated by results of MD simulations. This is the first identification of mechanistic control of the protonation state of flavin intermediates in a nucleophilic flavin-dependent monooxygenase.

Results

Reaction in the wild-type Lux:FMNH$^-$ complex with oxygen at various pH values: identification of the pK_a associated with the flavin C4a-OOH

It is not known whether after reacting the reduced enzyme-bound $FMNH^-$ with O_2, the first species formed is the flavin C4a-OOH or the flavin C4a-OO$^-$. If it is the former, removal of a proton would be required to yield the flavin C4a-OO$^-$, which is required for the subsequent reaction with the aldehyde substrate. To distinguish these possibilities, the reactions of wild-type Lux:FMNH$^-$ with oxygen at various pH values were investigated using transient kinetics methods to identify spectroscopic changes attributable to deprotonation or protonation of the intermediate flavin–oxygen species. An anaerobic solution containing 18 μM FMNH$^-$ and 80 μM wild-type Lux was mixed with buffers containing 0.13 mM O_2 at various pH values (concentrations after mixing). The reaction was monitored by the absorbance changes at 380 nm and 446 nm to detect the formation of flavin C4a-OOH and oxidized flavin, respectively. Reactions at all pH values investigated showed three phases of flavin C4a-OOH intermediate formation (Fig. 1B) with the characteristics being dependent on pH. At low pH (pH 6–7.5), the first phase (dead time to 0.01 s) showed a rapid increase in absorbance at 380 nm, while the second (0.01–0.2 s) and third phases (0.2–10 s) showed only a small absorbance increase and decrease, respectively. At higher pH (8.0–9.5), the first

phase (dead time to 0.02 s) was also an increase in absorbance at 380 nm as found in the reactions at low pH, but the magnitudes were greater. The second (0.02–0.04 s) and third phases (0.04–10 s) showed small increase and decrease in absorbance 380 nm. When the same reaction was monitored at 446 nm, there was no significant change in absorbance, even up to 100 s (data not shown), indicating no formation of oxidized FMN.

When observed rate constants (k_{obs}) were calculated, the k_{obs} of the first phase was in range of 350–450 s^{-1}. The reaction at higher pH values appeared to start at a higher absorbance levels (Fig. 1B), probably because the reaction proceeds slightly faster at higher pHs, so that more of the oxygen reaction proceeded during the dead time period than at lower pH. As no significant change in absorbance at 446 nm was observed during the first 5 s, it can be concluded that the detected intermediate did not eliminate H_2O_2 from the flavin C4a-OOH to form oxidized FMN (Scheme 1). To confirm that the first phase is due to the direct oxygen reaction, the reaction of Lux:FMNH$^-$ and oxygen at pH 7.0 was carried out with various oxygen concentrations. The only rate constants that were dependent on oxygen concentrations were those of the first phase with the second-order rate constant of 2×10^6 M^{-1}·s^{-1}; the second and third phases were not dependent on oxygen concentration (Fig. S1). The data imply that the first phase is a bimolecular reaction of enzyme-bound reduced flavin and oxygen to form the flavin C4a-OOH. Therefore, referring to the pH-dependent experiment, we speculated that after the first intermediate was formed, the second phase was due to the pH-dependent deprotonation of the C4a intermediate, resulting in a small increase in absorbance at 380 nm. At high pH, the first and second phases appear to merge. A plot of the absorbance change at 380 nm due to the first phase by 0.01 s *versus* pH was sigmoidal and associated with a pK_a of 7.7 ± 0.2 (Fig. 1C).

Determination of flavin C4a-OOH intermediate spectra at various pH values: assignment of flavin C4a-OOH as the first intermediate formed in the Lux reaction

To identify the spectral characteristics of the putative flavin C4a-OOH and C4a-OO$^-$ intermediates, stopped-flow experiments were performed as described in the previous section but using a diode array detector. Reactions were carried out by mixing a solution of Lux in 10 mM sodium phosphate pH 7 with an air-saturated solution of 100 mM buffer at various pH

values. At pH 7.08 (pH after mixing), the first intermediate spectrum detected at 0.005 s had a λ_{max} of 385 nm. This intermediate converted into a second species with a λ_{max} of 375 nm within 1 s (Fig. 2A). This time frame is consistent with the second and third phases shown in Fig. 1B. When the experiment was carried out at a final pH of 9.8, the first detected spectrum at 0.005 s had a λ_{max} of ~ 375 nm (data not shown). As the pH varied from pH 6.2 to 9.8 the λ_{max} of intermediate spectra observed at 0.01 s shifted from 385 to ~ 375 nm (Fig. 2B). These data suggest that the intermediate with a λ_{max} of 385 nm observed at low pH is associated with the protonated form, flavin C4a-OOH, and the intermediate with a λ_{max} of 375 nm found at high pH is associated with the deprotonated form. Thus, the first observed intermediate in the Lux reaction is most likely the flavin C4a-OOH, which then deprotonates to form the flavin C4a-OO⁻. No distinct fluorescence signal could be detected during the time period of converting flavin C4a-OOH to C4a-OO⁻ (0.001–1 s) (data not shown).

The dependence on pH of the intermediate spectra at 0.01 s yields an apparent pK_a of 8.1 ± 0.2 (Inset of Fig. 2B). This value agrees well with the apparent pK_a value calculated from the dependence on pH of the amplitude change in the first phase at 0.01 s monitored at 380 nm (Fig. 1C), indicating that the pK_a values calculated from the two experiments are due to the same species and are associated with the protonation state of the flavin C4a-OOH intermediate.

Identification of species required for light emission

Reactions of Lux:FMNH⁻ and oxygen at pH 8.0 in the presence of aldehyde (C10) were carried out to test whether the first intermediate with λ_{max} of 385 nm (presumably flavin C4a-OOH) could directly lead to light emission. Flavin C4a-OOH—*in principle*—is not expected to nucleophilically attack the aldehyde to form the corresponding acid and the excited state of the C4a-hydroxyflavin, the species that is thought to emit light. Figure 3 shows that at all pH values, no luminescence was produced until after the first intermediate had converted into the second intermediate (by about 0.1 s), presumably from the change in flavin C4a-OOH to the flavin C4a-OO⁻. It is speculated that in the time frame of 0.1 to 1.0 s, corresponding to the third phase of absorbance change at 380 nm (blue line in Fig. 3), as flavin C4a-COO⁻ is progressively generated, reaction with aldehyde generates the C4a-peroxy-hemiacetal required for light generation reaction and possibly a small quantity of the excited state of the C4a-hydroxyflavin is generated. The latter species seems to continue to form until ~ 25 s, corresponding to the maximum intensity of light emission and to the formation of decanoic acid. It should be pointed out that the integrated light emission occurring between 0.1 and 1.0 s is extremely small compared with that occurring from about 10 to 400 s. The logarithmic *x*-axis visually emphasizes the early portion of light
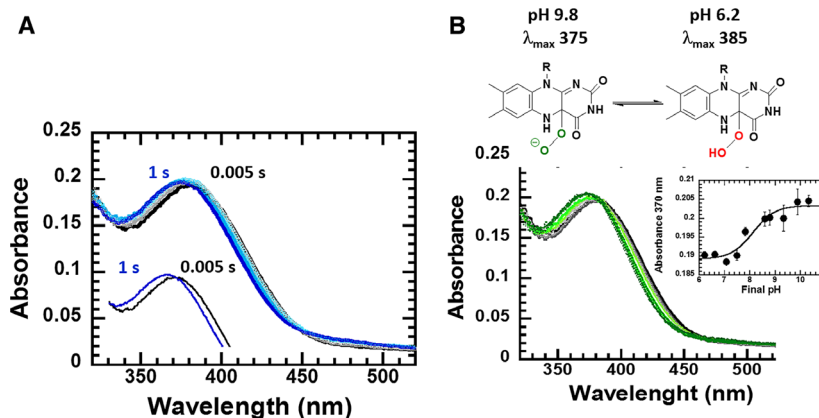

Fig. 2. Spectra of the flavin C4a-OOH of wild-type Lux reaction at various pH values. Solutions of 80 μM Lux and 16 μM FMNH⁻ in 10 mM sodium phosphate buffer pH 7.0 were mixed with a buffer containing oxygen (0.13 mM) at various pH values at 4 °C. Intermediate spectra were recorded by a diode array detector on the stopped-flow spectrophotometer. (A) Spectra of the flavin C4a-OOH of the wild-type Lux at final pH of 7.0 were detected at different time points. (B) The spectra of the flavin C4a-OOH monitored at 0.01 s at various reaction pH values. Inset of (B) A plot of absorption at 370 nm of (B) *versus* pH shows that the observed species is associated with a pK_a of 8.1 ± 0.2. The reactions were performed in triplicate and presented as mean ± standard deviation.

Fig. 3. Comparison of the kinetics observed at pH 8 of both the absorbance at 380 nm and light emission. Kinetic traces were obtained from single turnover reactions of Lux:FMNH$^-$ (80 μM Lux and 16 μM FMNH$^-$) reacting with oxygen in air-saturated buffers containing 20 μM decanal at 4 °C. The reaction was monitored at absorbance 380 nm (blue line), and light emission was detected by a photomultiplier tube attached to the stopped-flow instrument (purple line). The spectrum at 0.005 s corresponds to the flavin C4a-OOH intermediate of 385 nm. During this period, no light is generated. As the 385 nm intermediate gradually deprotonates to form the flavin C4a-OO$^-$ with a λ_{max} of 375 nm, light emission begins as the flavin C4a-OO$^-$ reacts with the aldehyde substrate resulting in formation of the light-emitting excited state flavin C4a-hydroxide.
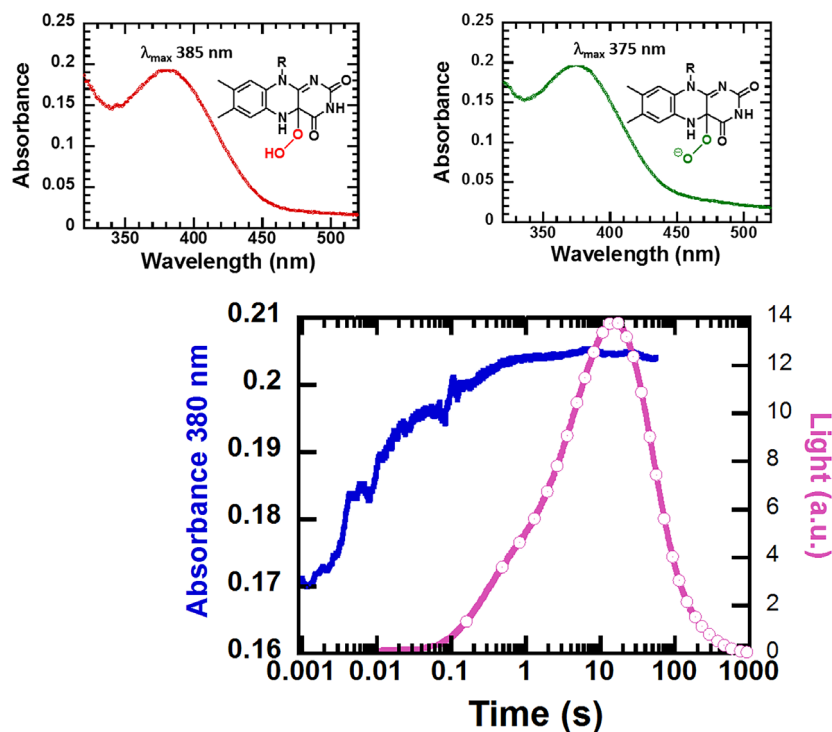
emission. All the above results are consistent with the first intermediate being the flavin C4a-OOH and the second intermediate as the flavin C4a-OO$^-$ and that the latter is the species reacting with the aldehyde to eventually form the acid and the light-emitting species.

The pH dependence of total light emission had a bell-shaped profile (Fig. S2) with an optimum near pH 7. There is an apparent pK_a of ~ 5.2 for a group required to be deprotonated for efficient light emission and a pK_a of ~ 8.6 for further deprotonation resulting in decreased light emission. The observed apparent pK_a could be due to the Baeyer–Villiger step of attacking the aldehyde or to the generation of the acid product to form the excited state of the C4a-hydroxyflavin or to other factors such as change in protein structure at very low and high pH values. And light emission efficiency might not be related to the observed pK_a of the terminal peroxy group of flavin C4a-OOH intermediate.

Identification of His44 as an important residue for generating flavin intermediates required for light emission

A recent computational investigation of the oxygen activation mechanisms in Lux predicted that the His44 residue nearby the C4a position serves as a strategic proton donor, allowing formation of the flavin C4a-OOH in the active sites [33]. We therefore tested whether the active site His in Lux indeed also facilitates the formation and controls the protonation state of the flavin C4a-OOH. Two His residues, His44 and His45, were identified to be located close to the C4a position of FMN (Fig. 1A). We constructed His44 and His45 variants, replacing them with Ala, Asn, and Asp, and compared their bioluminescence activities with those of the wild-type enzyme. The assay reaction was performed using the C$_1$ flavin reductase to continuously generate FMNH$^-$ as a substrate for Lux [21,22]. All variants exhibited very low bioluminescence and could be classified as dim phenotypes (Table 1). Stopped-flow experiments of the reaction of O$_2$ with the reduced forms of the His44 variants (His44Ala, His44Asn, and His44Asp) were carried out

Table 1. The total light emission in Lux wild-type and mutant enzymes.

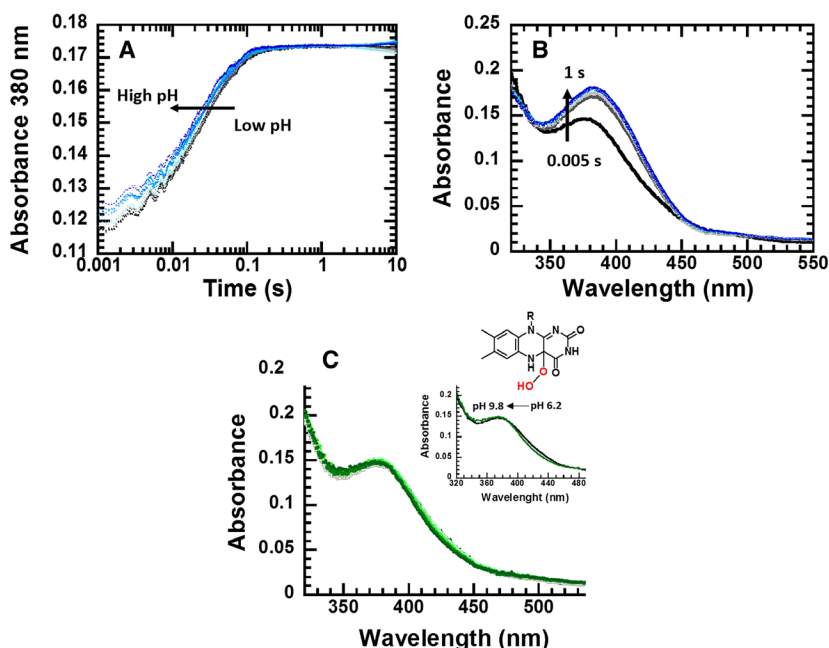| Enzyme	Total light emission (arbitrary unit)	Relative activity (%)
Wild-type	2.82 $\pm$ 0.016	100
His44Ala	0.04 $\pm$ 0.010	1.56
His44Asp	0.06 $\pm$ 0.003	2.12
His44Asn	0.06 $\pm$ 0.008	2.20
His45Ala	0.05 $\pm$ 0.003	1.73
His44Ala/ His45Ala	0.04 $\pm$ 0.001	1.95

Fig. 4. (A) The kinetic traces monitored at 380 nm of Lux:FMNH$^-$ and oxygen reaction of His44Ala at various pH values. Solutions of 80 μM Lux His44Ala and 16 μM FMNH$^-$ in 10 mM sodium phosphate buffer pH 7.0 were mixed with oxygen (0.13 mM after mixing) containing buffers at various pH values at 4 °C. (B) Spectra of the flavin C4a-OOH of His44Ala at final pH of 7.0 were detected at various time points. (C) Spectra of the flavin C4a-OOH at 0.005 s at various reaction pHs. Inset of C, same as (C) except that it shows the reaction at pH 6.2 (black) and 9.8 (green).

as those for the wild-type enzyme described in Fig. 1B. All of the variants could form the flavin C4a-OOH, as the increase in the absorbance 380 nm could be clearly detected. However, the kinetics of formation of the intermediates in the variants was distinctively different from that of the wild-type enzyme. Only a single somewhat slower phase of flavin C4a-OOH formation was observed. In contrast to the behavior of the wild-type enzyme, the kinetics and spectral characteristics of the intermediate had very little dependence on the reaction pH (Fig. 4) over the range 6–10.6, indicating that the intermediate formed did not change in protonation state.

The above data suggest that the oxygen reaction in His44Ala forms the flavin C4a-OOH without subsequent deprotonation. The observed rate constant for formation of the intermediate at 130 μM O$_2$ was around 68–70 s^{-1} at pH 7.0 and dependent on oxygen concentrations in a second-order fashion (Fig. 4A and Fig. S3). A second-order rate constant of ~ 0.2 × 10^6 M^{-1}·s^{-1} was calculated, about 10% of that for wild-type Lux. The intermediate spectrum of His44Ala at 0.005 s had a λ_{max} of 385 nm; no changes in the spectra were observed as the reaction progressed until after ~ 1 s at any of pH values investigated (Fig. 4B,C). The spectral characteristics of the intermediate in His44Ala are very similar to those of the flavin C4a-OOH species in wild-type Lux (Fig. 2B at low pH), consistent with His44Ala Lux only forming the flavin C4a-OOH, which remains protonated throughout the reaction. Because the flavin C4a-OOH

generated is not a sufficiently strong nucleophile to react with an aldehyde substrate, it cannot form the acid and the excited state C4a-hydroxyflavin intermediate, and thus, His44Ala exhibits a dim phenotype (Table 1). When the same experiments were carried out with the His44Asn and His44Asp variants, similar spectral intermediates with λ_{max} values of 385 nm were found, and the spectra remained nearly stable at all pH values with λ_{max} only slightly shifting to ~ 380 nm at pH 9–10.5 (Figs S4 and S5). These results indicate that the three His44 variants, especially His44Ala only form the flavin C4a-OOH as an intermediate in the reaction of their reduced forms with O$_2$.

Rate of H$_2$O$_2$ elimination as an indicator to identify the flavin C4a-OOH protonation status

Previous results with P2O and C$_2$ indicated that proper interactions between the N5 position of the flavin C4a-OOH intermediate and active site residues are important for stabilizing the flavin C4a-OOH [31,40,41]. In these enzymes, in which the flavin C4a-OOH is quite stable, increasing pH increases the rate of H$_2$O$_2$ elimination, suggesting that the protonated form is more stable than the peroxide form [26,31,42]. However, as shown in Fig. 1B, the flavin C4a-OOH in the wild-type Lux can be deprotonated, and the resulting species is quite stable (Scheme 2). Figure 5 shows results from measurements of the decay of the C4a intermediate as monitored by the absorbance at 446 nm, which indicates the formation of oxidized
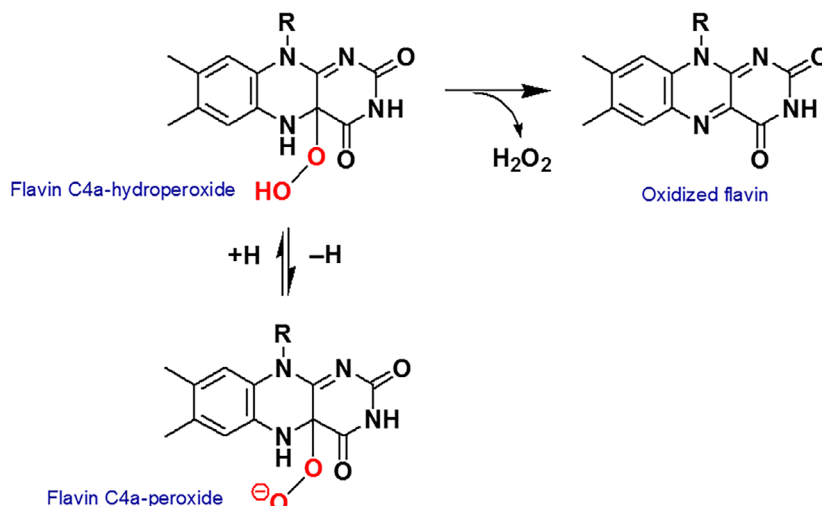
Scheme 2. Different protonation states of flavin-C4a-OOH intermediates and the elimination of H_2O_2 from the flavin-C4a-OOH to form oxidized flavin and H_2O_2.
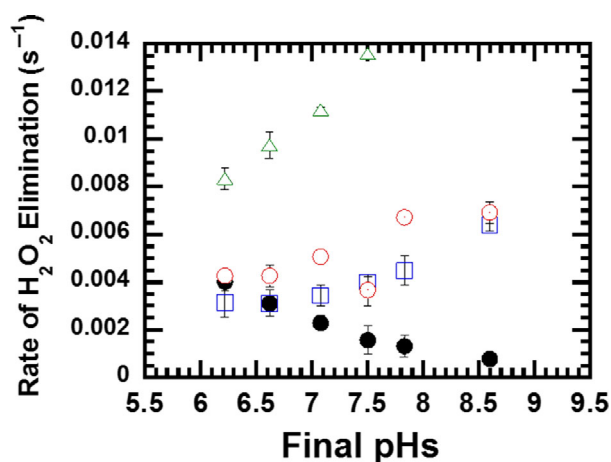

Fig. 5. Dependence on pH of observed rate constants for elimination of H_2O_2 from the flavin C4a-OOH to form oxidized FMN for wild-type (filled circles) and His44 mutants (empty squares, His44Ala; empty circles, His44Asp; empty triangles, His44Asn). The reactions were carried out in triplicate and presented as mean ± standard deviation.

FMN. With wild-type Lux, increasing the pH from 6.5 to 9 actually results in slower decay of the intermediate. However, when the reaction pH was above pH 9, the rate of H_2O_2 elimination increased significantly (data not shown). This might be due to partial enzyme denaturation, causing release of the flavin intermediate, so the flavin would become exposed to solvent where H_2O_2 is rapidly eliminated.

The elimination of H_2O_2 from the intermediates of the His44 variants (His44Ala, His44Asn, and His44Asp) had different pH-rate profiles from those of

wild-type Lux. Increasing the pH led to increasing rates of H_2O_2 elimination from these variants, analogous to those reported for C_2 and P2O reactions mentioned above. It suggests that the flavin C4a-OO$^-$ formed in the wild-type Lux is more stable than the flavin C4a-OOH of the variants. Furthermore, it is likely that these variant proteins are somewhat less structurally stable than the wild-type and that they might expose the flavin C4a-OOH to solvent at higher pH more readily than does wild-type. This would lead to a more rapid formation of oxidized FMN.

Reaction of the His45Ala variant with oxygen: His45 is important for FMNH$^-$ binding

When the reaction of the His45Ala:FMNH$^-$ complex was mixed with an oxygen (air-saturated) containing solution and monitored at 380 and 446 nm, kinetic traces at both wavelengths showed no evidence of a flavin C4a-OOH intermediate forming but only an autocatalytic increase in absorbance that was complete by ~ 2 s (Fig. S6). These reaction characteristics are essentially the same as those for the reaction of free FMNH$^-$ with oxygen [42], indicating that the His45Ala variant does not bind the FMNH$^-$ under the conditions employed. Therefore, the FMNH$^-$ binding properties of the His45Ala variant were examined to compare with those of the wild-type enzyme. The K_d value of FMNH$^-$ binding to His45Ala variant was calculated to be 370 ± 10 µM, which was approximately 58-fold greater than that of the wild-type enzyme (6.44 ± 0.53 µM) (Fig. 6A), indicating that the FMNH$^-$ binding of the His45Ala variant is impaired. Molecular dynamics (MD) [43–46] simulations were also carried out using the NAMD program [47] to
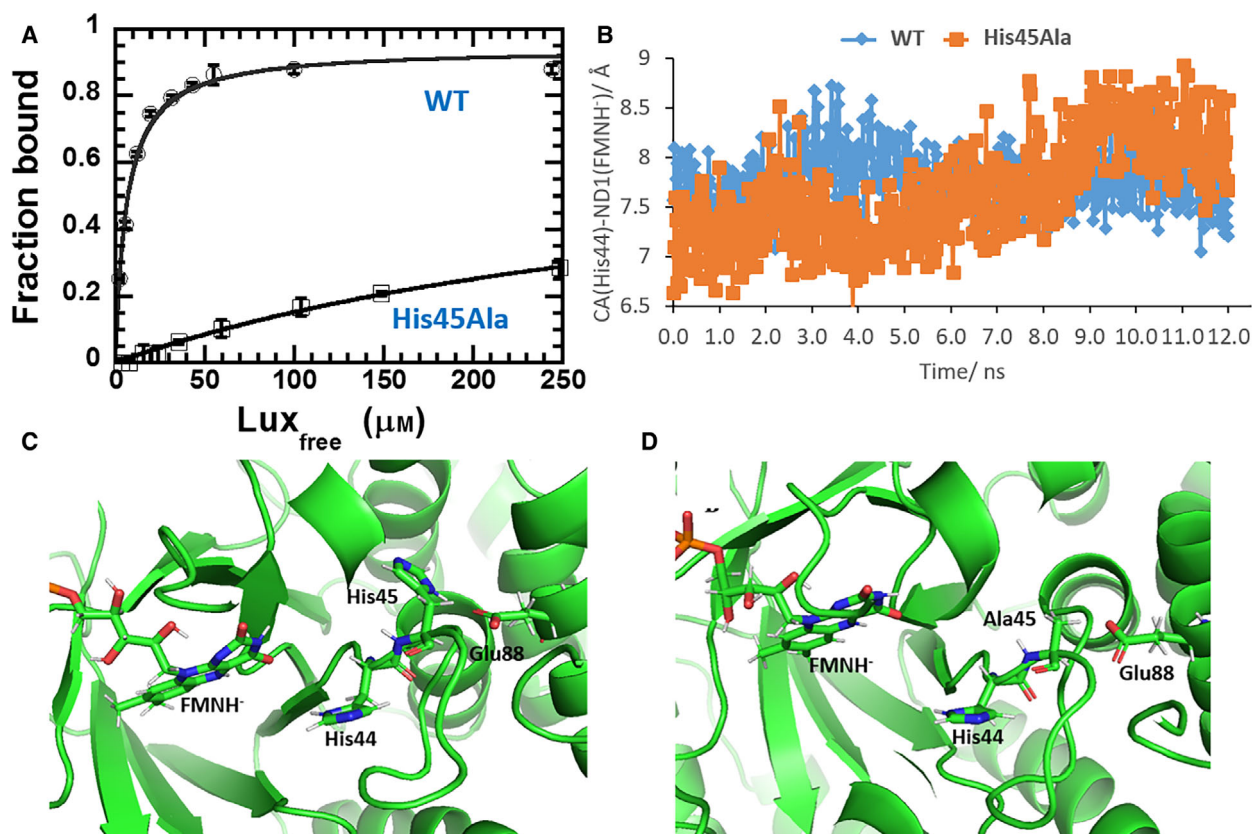
Fig. 6. Results from FMNH$^-$ binding experiments of wild-type and His45Ala Luxs. The K_d values were calculated to be 6.44 $\pm$ 0.53 µM and 370 $\pm$ 10 µM, respectively (A). The binding reactions were performed in triplicate and presented as mean $\pm$ standard deviation. Comparison of the distances obtained from MD simulations between wild-type and His45Ala of CA(His44)-ND1(FMNH$^-$) in (B). Snapshots obtained during 12-ns MD simulations of Lux wild-type (C) and His45Ala (D) with FMNH$^-$ show relative movements of the position of residues in the enzyme active sites. The pictures in (C) and (D) were created by PYMOL program (Schrödinger Inc.).

gain insights into the structural features that govern the overall process. The wild-type Lux enzyme structure from the Protein Databank (PDB) with code 3FGC was used in the analysis [12]. The Lux structure was first solvated in a theoretical box of TIP3P water. The temperature of the system was increased, and the system was equilibrated and further monitored for 12 ns. For the His45Ala, the three-dimensional structure of the variant was created using CHARMM and a similar MD analysis was carried out as for the wild-type enzyme. The data of the wild-type enzyme were used to measure the distance between an alpha carbon of His44 and the N1 position of FMNH$^-$ (CA(His44)-ND1(FMNH$^-$)). The MD simulations data indicate that the CA(His44)-ND1(FMNH$^-$) (Fig. 6B) distances increase during 12-ns MD simulations for His45Ala, while those of wild-type did not increase. Snapshots of the wild-type and His45Ala during 12-ns MD simulations are depicted in Fig. 6C,D, respectively.

Furthermore, the distances of the alpha carbons of His44 and Tyr110 (CA(His44)-CA(Tyr110)) and the alpha carbons of His44 and Glu88 (CA(His44)-CA (Glu88)) of the wild-type enzyme (8–10.0 Å) are more stable and closer for the wild-type than that of His45Ala (9.5–10.5 Å) (Fig. S7). These results indicate that FMNH$^-$ is bound more stably in wild-type Lux than in the His45Ala variant. The longer distance between FMNH$^-$ and active site residues in the His45Ala would cause more fluctuation in the flavin binding, which may lower binding affinity and cause the losing of FMNH$^-$ binding (high K_d of the binding). These results are consistent with the experimental data reported above (Fig. 6).

Discussion

This report has elucidated the protonation status of Lux flavin C4a-OOH intermediates during the course

of the catalytic reaction. It has identified the essential role of His44 in controlling the deprotonation of the flavin C4a-OOH for chemical catalysis plus the role of His45 for FMNH$^-$ binding. The results also indicate that the first intermediate formed upon reacting oxygen with Lux:FMNH$^-$ is flavin C4a-OOH that deprotonates to form C4a-OO$^-$, which is required for light emission. Understanding how the protonation of flavin C4a-OOH can be controlled is important for fine-tuning the activity of nucleophilic or electrophilic monooxygenases.

The protonation status of Lux flavin C4a-adduct intermediates can be identified using the changes in spectroscopic properties. Different protonation states of flavin C4a-OOH result in different wavelength maxima. Previously, it was shown that C4a-OO$^-$ in some systems has a shorter λ_{max} than that of the flavin C4a-OOH [29,34,48,49]. In CHMO, the first intermediate detected is the deprotonated form with λ_{max} around 366 nm, which then interconverts with the rate constant of 3 s^{-1} to an intermediate with λ_{max} of 383 nm assigned as flavin C4a-OOH [34]. The Lux reaction was different from the CHMO reaction in that the first intermediate formed was the flavin C4a-OOH. Deprotonation of this species is most likely required for the C4a-adduct to attack the aldehyde and produce the acid and the excited state flavin hydroxide necessary for light emission. His44 was shown to be important for this deprotonation to occur. The λ_{max} of flavin C4a-OOH species in siderophore-associated flavin monooxygenase [48], ornithine hydroxylase [49], phenol hydroxylase [50], and 3-hydroxybenzoate-6-hydroxylase was also found to be pH-dependent [51].

The Lux flavin C4a-OOH intermediate pK_a was determined to be 7.7–8.1 (Figs 1C and 2B). This value is comparable to the pK_a value assigned for deprotonation of flavin C4a-OOH in the CHMO reaction as 8.4 [34]. However, in electrophilic monooxygenases, for example, *p*-HPA hydroxylase, the acid/base pK_a is thought to be as high as 9.8. This enables these flavin-dependent monooxygenases to keep the reactive form of the C4a-flavin intermediate over a wide range of pH for electrophilic substitution [26,29]. Because His44 is an important residue for facilitating deprotonation of the flavin C4a-OOH, it is possible that a pK_a of 7.7–8.1 is associated with the pK_a of His44 (Fig. 7), in which the imidazole ring gets protonated by abstracting the proton from flavin C4a-OOH. However, the pH-activity profile for light emission of Lux was bell-shaped with an optimum pH around 7 (Fig. S2), suggesting that other dissociable protons and stabilization of protein structures are also important for light emission. In addition, in the pH-activity profile experiment, the presence of aldehyde in the enzyme active site may also influence the pK_a of the flavin C4a-OOH intermediate and the dissociable groups related to the steps of nucleophilic attack, the formation of flavin C4a-peroxyhemiacetal and O–O bond breaking to generate excited C4a-hydroxyflavin to liberate light.

We propose that the function of His44 is to abstract a proton to generate the flavin C4a-OO$^-$, making the intermediate ready for participating in the nucleophilic attack on the aldehyde substrate (Fig. 7). The replacement of a potential active site base in the His44Asp variant could not restore the activity (Table 1). Apparently, the aspartate residue is too acidic to abstract the
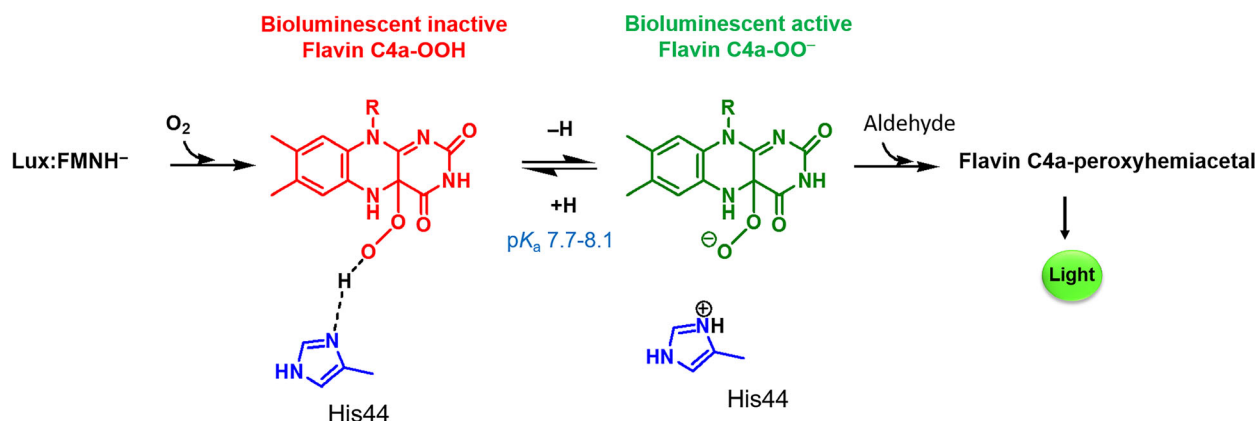

Fig. 7. His44 functions as a key catalytic residue to facilitate the formation of the light active intermediate of flavin C4a-OO$^-$ in the Lux reaction. The intermediate is first generated as the protonated flavin C4a-OOH, which is a light-inactive intermediate, as it cannot react with an aldehyde. The active site His44 residue abstracts the hydroperoxide proton to generate the light active flavin C4a-OO$^-$, which nucleophilically attacks aldehyde, allowing the ensuing bioluminescence reaction.

hydroperoxide proton. Thus, without the imidazole ring in the His44 variants, the C4a-intermediate remains as the flavin C4a-OOH and is unable to react with aldehyde to generate the excited C4a-hydroxyflavin and acid product. This is firmly supported by the finding of drastically reduced bioluminescence with essentially no conversion of aldehyde to acid in the His44Ala variant of Lux from *V. harveyi* [37]. Our results are also in accordance with a previous report where it was suggested that His44 in the Lux active site functions as a catalytic acid in providing a proton for the first flavin C4a-OOH formation [33]. For the formation rates of flavin C4a-OOH in the His44, mutants are four- to fivefold slower than that of the wild-type. However, because the flavin C4a-OOH does form in the His44 variants suggests that in the absence of His44, a proton from His45 or from the outside environment may protonate the flavin intermediate [29]. Coupling the present results and those from the MD calculations [33], the active site His44 in Lux may function to shuttle protons by first providing a proton during the flavin C4a-OOH formation and then abstracting a proton back to form the flavin C4a-OO$^-$.

The pH-rate dependence of H_2O_2 elimination from the C4a adduct of Lux also suggests that in the His44 variants, the protonated flavin C4a-OOH exists throughout the range of pH investigated because the rate of H_2O_2 elimination increases with increasing pH similar to the cases of other enzymes that are known to have their intermediates protonated (C_2 [26,41] and P2O [31,40]). As the terminal -OOH in flavin C4a-OOH in these systems can serve as a proper leaving group, the increased pH facilitates H_2O_2 elimination by increasing the rate of N5-H dissociation (Scheme 2) [23,40,41]. For the reaction of wild-type Lux, the pH-rate profile of H_2O_2 elimination is different because the lower pK_a of the flavin C4a-OOH favors the C4a-OO$^-$ form (or possibly the higher pK_a of the His44). Possibly, the hydrophobic environment provided by Leu41 and Leu42 close to proposed flavin C4a-OO$^-$ might help to stabilize this form of intermediate [12].

Although located nearby, His45 is also important for the Lux light-emitting reaction but with a different role. Experimental results and MD simulations of FMNH$^-$ binding have indicated the importance of His45 for flavin binding. The previously reported results of His45 variants also agree well with our current data. Changing His45 to Cys, Gln, or Ser residues in Lux from *V. harveyi* resulted in a dark phenotype of the enzyme [39]. In the crystal structure, the His45 residue was found to form a H-bond with Glu88 from the β-subunit located in the subunit interface [13]. The interaction of the amino acids at the α,β subunit interface is crucial for the light reaction. The disruption of

the H-bond interaction in the His45Ala variant could affect the active conformation of the α-subunit to impair the FMNH$^-$ binding, and this would prevent catalysis and light emission.

In conclusion, we have shown that the reaction of Lux:FMNH$^-$ with O_2 forms flavin C4a-OOH as the first intermediate, and the deprotonation process that is controlled by His44 takes place to generate the active intermediate flavin C4a-OO$^-$. The understanding of how the deprotonation of flavin C4a-OOH can be affected is important for future rational enzyme engineering to fine-tune reactivities of nucleophilic or electrophilic flavoprotein monooxygenases.

Materials and methods

Chemicals and reagents

All laboratory reagents used were analytical grade. High-purity FMN was obtained by hydrolysis of FAD with snake venom phosphodiesterase according to the method described in Ref. [52]. All chromatographic media were obtained from GE Healthcare (Bronx, NY, USA). The molecular reagents were obtained from New England Biolab (Ipswich, MA, USA). The extinction coefficients at pH 7.0 of the following compounds were used for determining their concentrations: NADH ε_{340} = 6.22 mM^{-1}·cm^{-1}; FMN ε_{450} = 12.2 mM^{-1}·cm^{-1}; and flavin-dependent reductase from *Acinetobacter baumannii*, C_1 ε_{450} = 12.8 mM^{-1}·cm^{-1}, Lux (wild-type and mutants) ε_{280} = 79.6 mM^{-1}·cm^{-1}.

Site-directed mutagenesis

Site-directed mutagenesis to create His44 and His45 variants was performed using the QuikChange II Site-Directed Mutagenesis Kit (Agilent Technologies, Santa Clara, CA, USA). The pET11a plasmid carrying Lux from *Vibrio campbellii* wild-type (pET11a-Lux) was used as a template for mutagenic PCR using the GeneAmp PCR System (Applied Biosystems, Carlsbad, CA, USA). The sequences were confirmed by DNA sequencing (Macrogen Inc., Seoul, Korea).

Protein expression and purification

The plasmid pET11a-Lux carrying the wild-type and mutants genes was transformed into *Escherichia coli* BL(21) DE3 to overexpress the proteins. The procedures for overexpression and purification of proteins were carried out according to methods described in Ref. [21].

Enzyme assays

The luciferase assay was carried out by coupling the Lux reaction with the reduction in FMN by the flavin reductase

of *p*-HPA hydroxylase from *A. baumannii* (C₁) [53]. A rapid-mixing apparatus (Model SFA-20, TgK Scientific, Bradford-on-Avon, UK) was used to mix the reaction components at 25 °C before light emission was monitored over time using a spectrofluorometer (Cary Eclipse, Varian Inc., Mulgrave, Australia). Light emission was measured at 490 nm with a slit width of 5 nm. The assays included 20 μM FMN, 100 μM HPA, 2 μM Lux, 2–4 μM C₁, 100 μM NADH, and 40 μM dodecanal (freshly prepared in methanol) and were conducted in 50 mM sodium phosphate buffer pH 7.0. The enzyme activity was presented as total light emission calculated from the peak area underneath the emission trace using arbitrary units. The effect of pH on light emission of Lux was investigated by assaying enzyme (4 μM) activity in 50 mM buffer at pH 5.5–10. Sodium acetate buffer was used for maintaining pH 5.5, sodium phosphate buffer for pH 6.0–8.0, Tris/H₂SO₄ buffer for pH 8.5, and glycine/NaOH for pH 9–10.

Transient kinetics studies of the Lux reaction

Transient kinetics studies were performed using a stopped-flow spectrophotometer (Model 300E; TgK Scientific) in single mixing mode with a 1 cm optical path length observation cell. Flow path of the stopped-flow apparatus was made anaerobic by flushing the system with anaerobic buffer and replacing with an oxygen scrubbing solution overnight. The scrubbing solution was either a solution of 400 μM protocatechuic acid (PCA) and 1 μg·mL⁻¹ protocatechuic acid dioxygenase (PCD) from *Burkholderia cepacia* [54] or a solution of 5 mg·mL⁻¹ sodium dithionite in 50 mM sodium phosphate buffer pH 7.0. Before performing experiments, the flow path was thoroughly washed with an anaerobic solution of working buffer. The anaerobic solution of Lux:FMNH⁻ (160 μM Lux from *V. campbellii* and 32 μM FMN) in 10 mM sodium phosphate buffer pH 7.0 was prepared in an anaerobic glove box (Belle Technology, Weymouth, UK) by reducing the FMN with aliquots of ~ 10 mM sodium dithionite (in 100 mM potassium phosphate, pH 8.0) and monitoring spectrophotometrically. The solution was then transferred into a glass tonometer before being loaded onto the stopped-flow instrument. The anaerobic solution containing Lux:FMNH⁻ in the first syringe was mixed with an equal volume of a solution containing oxygen (air-saturated concentration, 0.26 mM) in various pH buffers (100 mM sodium phosphate buffer pH 6.0–7.0, 100 mM Tris/H₂SO₄ buffer pH 7.5–8.5, and 100 mM glycine/NaOH pH 9.0–10.5). The reactions were monitored using photomultiplier detection to monitor absorbance changes at 380 and 450 nm. Observed rate constants for flavin C4a-OOH intermediate formation and H₂O₂ elimination at various pH values were calculated from the absorbance changes occurring over time at 380 and 450 nm. A pK_a value that is associated with the conversion between protonated and deprotonated forms of flavin C4a-OOH

was determined by correlating the spectral characteristics of flavin C4a-OOH and flavin C4a-OO⁻ as a function of pH. In these latter experiments, spectra of intermediates at various pH values were monitored by a diode array detector attached in the stopped-flow spectrophotometer. Light emission kinetics were performed by mixing Lux:FMNH⁻ with an air-saturated buffer containing 40 μM decanal. Light was monitored by the photomultiplier tube attached to the stopped-flow spectrophotometers with lamp off mode. Kinetic data were analyzed using Program A, which was developed by C.J. Chiu, R. Chang, J. Diverno, and D.P. Ballou at the University of Michigan. Specific details of individual experiments are described in figure legends and in the text.

FMNH⁻ binding properties

The determination of FMNH⁻ binding properties of Lux enzyme was employed according to methods described in Ref. [18]. In brief, an anaerobic FMNH⁻ solution (7 μM) in 50 mM sodium phosphate pH 8.0 was mixed with air-saturated buffer containing various concentrations of Lux (0–250 μM) at 4 °C in the stopped-flow spectrophotometer. The reoxidation of FMNH⁻ was monitored by absorbance at 446 nm. The fractions of enzyme-bound FMNH⁻ used for K_d value calculations were obtained from the differences in the amplitude changes in the absorbance 446 nm between the reactions in the absence and presence of the Lux enzyme.

Computational details

A three-dimensional model of Lux was obtained from the Protein Databank (PDB: 3FGC) [11]. This structure is a crystal structure of the Lux co-crystallized with FMN, at a resolution of 2.3 Å. Hydrogen atoms of amino acid residues were added according to the results from the PROPKA program [40]. The atom types in the topology files were assigned on the basis of the CHARMM27 parameter set [41]. The structure of the Lux enzyme was theoretically solvated in a cubic box of TIP3P water extending at least 15 Å in each direction from the solute. Dimensions of the solvated system were 88 × 116 × 102 Å. Molecular dynamics (MD) simulations were carried out using NAMD program [26,42,43]. The simulations were started by minimizing hydrogen atom positions for 3000 steps followed by water minimization for 6000 steps. The system water was heated to 300 K for 5 ps and then equilibrated for 15 ps. The whole system was minimized for 10 000 steps and heated to 300 K for 20 ps. After that, the entire system was equilibrated for 180 ps and followed by a production stage for 12 ns. To investigate the role of His45 in enzyme catalysis, molecular modeling of the His45Ala variant was also carried out. The same procedure as applied to the wild-type enzyme was applied to the

His45Ala variant. Distances between atoms of alpha carbons of His44 (CA(His44)) and the C4a position of FMNH$^-$ (C4A(FMNH$^-$)), CA(His44) and the N1 position of FMNH$^-$ (ND1(FMNH$^-$)), or the CA(His44) and alpha carbons of Glu88 (CA(Glu88)) during the MD simulations were measured.

Acknowledgements

Conflict of interest

The authors declare no conflict of interest.

Author contributions

RT performed experiments, designed the experiments, analyzed the results, and wrote the basic manuscript. NL designed and performed computational calculations and contributed to writing the manuscript. NA, PP, and WC performed enzyme preparation and transient kinetics of fluorescence and pH-dependent bioluminescence experiments. CS performed preliminary experiments. JS and P. Chenprakhon gave suggestions on the experimental design and data analysis. DPB and BE made substantial modifications to the writing and to the interpretation of results. P. Chaiyen conceived the study, helped to design the experiments, and contributed to the writing of the manuscript. All authors reviewed the results and approved the final version of the manuscript.

References

1 Shimomura O (2006) Bioluminescence: Chemical Principles and Methods, 1st edn. World Scientific Publishing Co. Pte. Ltd., Singapore.

2 Tinikul R & Chaiyen P (2016) Structure, mechanism, and mutation of bacterial luciferase. *Adv Biochem Eng Biotechnol* **154**, 47–74.

3 Ulitzur S (1997) Review paper established technologies and new approaches in applying luminous bacteria for analytical purposes. *J Biolumin Chemilumin* **121**, 79–192.

4 Francis KP, Joh D, Bellinger-Kawahara C, Hawkinson MJ, Purchio TF & Contag PR (2000) Monitoring bioluminescent *Staphylococcus aureus* infections in living mice using a novel *luxABCDE* construct. *Infect Immun* **68**, 3594–3600.

5 Brodl E, Winkler A & Macheroux P (2018) Molecular mechanisms of bacterial bioluminescence. *Comput Struct Biotechnol J* **16**, 551–564.

6 Meighen EA (1991) Molecular biology of bacterial bioluminescence. *Microbiol Mol Biol Rev* **55**, 123–142.

7 Mitiouchkina T, Mishin AS, Somermeyer LG, Markina NM, Chepurnyh TV, Guglya EB, Karataeva TA, Palkina KA, Shakhova ES, Fakhranurova LI *et al.* (2020) Plants with genetically encoded autoluminescence. *Nat Biotechnol* **38**, 1–3.

8 Close DM, Patterson SS, Ripp S, Baek SJ, Sanseverino J & Sayler GS (2010) Autonomous bioluminescent expression of the bacterial luciferase gene cassette (*lux*) in a mammalian cell line. *PLoS One* **5**, 1–12.

9 Close D, Xu T, Smartt A, Rogers A, Crossley R, Price S, Ripp S & Sayler G (2012) The evolution of the bacterial luciferase gene cassette (*lux*) as a real-time bioreporter. *Sensors* **12**, 732–752.

10 Gregor C, Gwosch KC, Sahl SJ & Hell SW (2018) Strongly enhanced bacterial bioluminescence with the *ilux* operon for single-cell imaging. *Proc Natl Acad Sci USA* **115**, 962–967.

11 Gregora C, Papea JK, Gwoscha KC, Gilata T, Sahla SJ & Hella SW (2019) Autonomous bioluminescence imaging of single mammalian cells with the bacterial bioluminescence system. *Proc Natl Acad Sci USA* **116**, 26491–26496.

12 Campbell ZT, Weichsel A, Montfort WR & Baldwin TO (2009) Crystal structure of the bacterial luciferase/flavin complex provides insight into the function of the β subunit. *Biochemistry* **48**, 6085–6094.

13 Fisher AJ, Thompson TB, Thoden JB & Baldwin TO (1996) The 1.5-Å resolution crystal structure of bacterial luciferase low salt conditions. *J Biol Chem* **271**, 21956–21968.

14 Xin X, Xi L & Tu S-C (1994) Probing the *Vibrio harveyi* luciferase β subunit functionality and the intersubunit domain by site-directed mutagenesis. *Biochemistry* **33**, 12194–12201.

15 Vervoort J, Muller F, Lee J, van den Berg WAM & Moonen CTW (1986) Identifications of the true carbon-13 nuclear magnetic resonance spectrum of the stable intermediate II in bacterial luciferase. *Biochemistry* **25**, 8062–8067.

16 Ghisla S & Massey V (1989) Mechanism of flavoprotein-catalyzed reactions. *Eur J Biochem* **181**, 1–17.

17 Palfey BA & McDonald CA (2010) Control of catalysis in flavin-dependent monooxygenases. *Arch Biochem Biophys* **493**, 26–36.

18 Huijbers MME, Montersino S, Westphal AH, Tischler D & van Berkel WJH (2014) Flavin dependent monooxygenases. *Arch Biochem Biophys* **544**, 2–17.

19 Bruice TC (1984) Oxygen-flavin chemistry. *Isr J Chem* **24**, 54–61.

20 Abu-Soud HM, Mullins LS, Baldwin TO & Raushel FM (1992) Stopped-flow kinetic analysis of the bacterial luciferase reaction. *Biochemistry* **31**, 3807–3813.

21 Suadee C, Nijvipakul S, Svasti J, Entsch B, Ballou DP & Chaiyen P (2007) Luciferase from *Vibrio campbellii* is more thermostable and binds reduced FMN better than its homologues. *J Biochem* **142**, 539–552.

22 Tinikul R, Thotsaporn K, Thaveekarn W, Jitrapakdee S & Chaiyen P (2012) The fusion *Vibrio campbellii* luciferase as a eukaryotic gene reporter. *J Biotechnol* **62**, 346–353.

23 Chaiyen P, Fraaije MW & Mattevi A (2012) The enigmatic reaction of flavins with oxygen. *Trends Biochem Sci* **37**, 373–380.

24 Chenprakhon P, Wongnate T & Chaiyen P (2019) Monooxygenation of aromatic compounds by flavin-dependent monooxygenases. *Protein Sci* **28**, 8–29.

25 Entsch B, Cole L & Ballou DP (2005) Protein dynamics and electrostatics in the function of p-hydroxybenzoate hydroxylase. *Arch Biochem Biophys* **433**, 297–311.

26 Ruangchan N, Tongsook C, Sucharitakul J & Chaiyen P (2011) pH-dependent studies reveal an efficient hydroxylation mechanism of the oxygenase component of *p*-hydroxyphenylacetate 3-hydroxylase. *J Biol Chem* **286**, 223–233.

27 Balke K, Kadow M, Mallin H, Saß S & Bornscheuer UT (2012) Discovery, application and protein engineering of Baeyer-Villiger monooxygenases for organic synthesis. *Org Biomol Chem* **10**, 6249–6265.

28 Malito E, Alfieri A, Fraaije MW & Mattevi A (2004) Crystal structure of a Baeyer-Villiger monooxygenase. *Proc Natl Acad Sci USA* **101**, 13157–13162.

29 Chenprakhon P, Trisrivirat D, Thotsaporn K, Sucharitakul J & Chaiyen P (2014) Control of C4a-hydroperoxyflavin protonation in the oxygenase component of p-hydroxyphenyl-acetate-3-hydroxylase. *Biochemistry* **53**, 4084–4086.

30 Visitsatthawong S, Chenprakhon P, Chaiyen P & Surawatanawong P (2015) Mechanism of oxygen activation in a flavin-dependent monooxygenase: a nearly barrierless formation of C4a-hydroperoxyflavin via proton-coupled electron transfer. *J Am Chem Soc* **137**, 9363–9374.

31 Wongnate T, Surawatanawong P, Visitsatthawong S, Sucharitakul J, Scrutton NS & Chaiyen P (2014) Proton-coupled electron transfer and adduct configuration are important for C4a-hydroperoxyflavin formation and stabilization in a flavoenzyme. *J Am Chem Soc* **136**, 241–253.

32 Alfieri A, Fersini F, Ruangchan N, Prongjit M, Chaiyen P & Mattevi A (2007) Structure of the monooxygenase component of a two-component flavoprotein monooxygenase. *Proc Natl Acad Sci USA* **104**, 1177–1182.

33 Luo Y & Liu Y-J (2019) Revisiting the origination of bacterial bioluminescence: a QM/MM study on oxygenation reaction of reduced flavin in protein. *ChemPhysChem* **20**, 405–409. https://doi.org/10.1002/cphc.201800970

34 Sheng D, Ballou DP & Massey V (2001) Mechanistic studies of cyclohexanone monooxygenase: chemical properties of intermediates involved in catalysis. *Biochemistry* **40**, 11156–11167.

35 Orru R, Dudek HM, Martinoli C, Pazmino DET, Royant A, Weik M, Fraaije MW & Mattevi A (2011) Snapshots of enzymatic Baeyer-Villiger catalysis oxygen activation and intermediate stabilization. *J Biol Chem* **286**, 29284–29291.

36 Brondani PB, Dudek HM, Martinoli C, Mattevi A & Fraaije MW (2014) Finding the switch: turning a baeyer−villiger monooxygenase into a NADPH oxidase. *J Am Chem Soc* **136**, 16966–16969.

37 Xin X, Xi L & Tu S-C (1991) Functional consequences of site-directed mutation of conserved histidyl residues of the bacterial luciferase α subunit. *Biochemistry* **30**, 11255–11262.

38 Huang S & Tu S-C (1997) Identification and characterization of a catalytic base in bacterial luciferase by chemical rescue of a Dark Mutant. *Biochemistry* **36**, 14609–14615.

39 Li H, Ortego BC, Maillard KI, Willson RC & Tu S-C (1999) Effects of mutations of the His45 residue of *Vibrio harveyi* luciferase on the yield and reactivity of the flavin peroxide intermediate. *Biochemistry* **38**, 4409–4415.

40 Sucharitakul J, Wongnate T & Chaiyen P (2011) Hydrogen peroxide elimination from C4a-hydroperoxyflavin in a flavoprotein oxidase occurs through a single proton transfer from flavin N5 to a peroxide leaving group. *J Biol Chem* **286**, 16900–16909.

41 Thotsaporn K, Chenprakhon P, Sucharitakul J, Mattevi A & Chaiyen P (2011) Stabilization of C4a-hydroperoxyflavin in a two-component flavin-dependent monooxygenase is achieved through interactions at flavin N5 and C4a atoms. *J Biol Chem* **286**, 28170–28180.

42 Sucharitakul J, Phongsak T, Entsch B, Svasti J, Chaiyen P & Ballou DP (2007) Kinetics of a two-component p-hydroxyphenylacetate hydroxylase explain how reduced flavin is transferred from the reductase to the oxygenase. *Biochemistry* **24**, 8611–8623.

43 Karplus M & Petsko GA (1990) Molecular dynamics simulations in biology. *Nature* **347**, 631–639.

44 Bocharov EV, Sobol AG, Pavlov KV, Korzhnev DM, Jaravine VA, Gudkov AT & Arseniev AS (2004) From structure and dynamics of protein L7/L12 to molecular switching in ribosome. *J Biol Chem* **279**, 17697–17706.

45 Day R & Daggett V (2007) Direct observation of microscopic reversibility in single-molecule protein folding. *J Mol Biol* **366**, 677–686.

46 Dodson GG, Lane DP & Verma CS (2008) Molecular simulations of protein dynamics: new windows on mechanisms in biology. *EMBO Rep* **9**, 144–150.

47 Phillips JC, Braun R, Wang W, Gumbart J, Tajkhorshid E, Villa E, Chipot C, Skeel RD, Kalé L & Schulten K (2005) Scalable molecular dynamics with NAMD. *J Comp Chem* **26**, 1781–1802.

48 Frederick RE, Ojha S, Lamb A & Dubois JL (2014) How pH modulates the reactivity and selectivity of a siderophore-associated flavin monooxygenase. *Biochemistry* **53**, 2007–2016.

49 Kathleen M, Meneely EW, Barr J, Martin Bollinger J Jr & Audrey LL (2009) Kinetic mechanism of ornithine hydroxylase (PvdA) from *Pseudomonas aeruginosa*: Substrate triggering of O_2 addition but not flavin reduction. *Biochemistry* **48**, 4371–4376.

50 Xu D, Ballou DP & Massey V (2001) Studies of the mechanism of phenol hydroxylase:mutants Tyr289Phe, Asp54Asn, and Arg281Met. *Biochemistry* **40**, 12369–12378.

51 Sucharitakul J, Tongsook C, Pakotiprapha D, van Berkel WJH & Chaiyen P (2013) The reaction kinetics of 3-hydroxybenzoate 6-hydroxylase from *Rhodococcus jostii* RHA1 provide an understanding of the *para*-hydroxylation enzyme catalytic cycle. *J Biol Chem* **288**, 35210–35221.

52 Sucharitakul J, Chaiyen P, Entsch B & Ballou DP (2005) The reductase of *p*-hydroxyphenylacetate 3-hydroxylase from *Acinetobacter baumannii* requires *p*-hydroxyphenylacetate for effective catalysis. *Biochemistry* **44**, 10434–10442.

53 Chaiyen P, Suadee C & Wilairat P (2001) A novel two-protein component flavoprotein hydroxylase *p*-hydroxyphenylacetate hydroxylase from *Acinetobacter baumannii*. *Eur J Biochem* **268**, 5550–5561.

54 Patil PV & Ballou DP (2000) The use of protocatechuate dioxygenase for maintaining anaerobic conditions in biochemical experiments. *Anal Biochem* **286**, 187–192.

Supporting information

Additional supporting information may be found online in the Supporting Information section at the end of the article.

Fig. S1. The reaction of Lux:FMNH⁻ (wild-type enzyme) and oxygen at various oxygen concentrations.

Fig. S2. pH profile of total light emission.

Fig. S3. Kinetic traces of the reaction of reduced His44Ala Lux with oxygen at 4 °C and pH 7.0 as monitored at 380 nm.

Fig. S4. The reaction of Lux:FMNH⁻ (His44Asn) with oxygen at various pH values.

Fig. S5. The reaction of Lux:FMNH⁻ (His44Asp) with oxygen at various pH values.

Fig. S6. The reaction of Lux:FMNH⁻ (His45Ala) with oxygen.

Fig. S7. Distances between selected residues of wild-type and His45Ala mutant monitored by 12 ns MD simulations of the Lux:FMNH⁻ complex.